



THE UNIVERSITY *of* EDINBURGH

Edinburgh Research Explorer

CADASIL Affects Multiple Aspects of Cerebral Small Vessel Function on 7T-MRI

Citation for published version:

Van Den Brink, H, Kopczak, A, Arts, T, Onkenhout, L, Siero, JCW, Zwanenburg, JJM, Hein, S, Hübner, M, Gesierich, B, Duering, M, Stringer, MS, Hendrikse, J, Wardlaw, JM, Joutel, A, Dichgans, M & Biessels, GJ 2022, 'CADASIL Affects Multiple Aspects of Cerebral Small Vessel Function on 7T-MRI', *Annals of Neurology*. <https://doi.org/10.1002/ana.26527>

Digital Object Identifier (DOI):

[10.1002/ana.26527](https://doi.org/10.1002/ana.26527)

Link:

[Link to publication record in Edinburgh Research Explorer](#)

Document Version:

Publisher's PDF, also known as Version of record

Published In:

Annals of Neurology

General rights













Copyright for the publications made accessible via the Edinburgh Research Explorer is retained by the author(s) and / or other copyright owners and it is a condition of accessing these publications that users recognise and abide by the legal requirements associated with these rights.

Take down policy

The University of Edinburgh has made every reasonable effort to ensure that Edinburgh Research Explorer content complies with UK legislation. If you believe that the public display of this file breaches copyright please contact openaccess@ed.ac.uk providing details, and we will remove access to the work immediately and investigate your claim.



CADASIL Affects Multiple Aspects of Cerebral Small Vessel Function on 7T-MRI

Hilde van den Brink, MSc  ^{1†}, Anna Kopczak, MD  ^{2†}, Tine Arts, PhD  ^{3†},
Laurien Onkenhout, MD,¹ Jeroen C.W. Siero, PhD ^{3,4}, Jaco J.M. Zwanenburg, PhD ³,
Sandra Hein, BSc,² Mathias Hübner, MSc,² Benno Gesierich, PhD,^{2,5}
Marco Duering, MD ^{2,5}, Michael S. Stringer, PhD ⁶, Jeroen Hendrikse, MD, PhD,³
Joanna M. Wardlaw, MD ⁶, Anne Joutel, MD, PhD ⁷, Martin Dichgans, MD,^{2,8,9} and
Geert Jan Biessels, MD, PhD,¹ on behalf of the SVDs@target group

Objective: Cerebral small vessel diseases (cSVDs) are a major cause of stroke and dementia. We used cutting-edge 7T-MRI techniques in patients with Cerebral Autosomal Dominant Arteriopathy with Subcortical Infarcts and Leukoencephalopathy (CADASIL), to establish which aspects of cerebral small vessel function are affected by this monogenic form of cSVD.

Methods: We recruited 23 CADASIL patients (age 51.1 ± 10.1 years, 52% women) and 13 age- and sex-matched controls (46.1 ± 12.6 , 46% women). Small vessel function measures included: basal ganglia and centrum semiovale perforating artery blood flow velocity and pulsatility, vascular reactivity to a visual stimulus in the occipital cortex and reactivity to hypercapnia in the cortex, subcortical gray matter, white matter, and white matter hyperintensities.

Results: Compared with controls, CADASIL patients showed lower blood flow velocity and higher pulsatility index within perforating arteries of the centrum semiovale (mean difference -0.09 cm/s, $p = 0.03$ and 0.20 , $p = 0.009$) and basal ganglia (mean difference -0.98 cm/s, $p = 0.003$ and 0.17 , $p = 0.06$). Small vessel reactivity to a short visual stimulus was decreased (blood-oxygen-level dependent [BOLD] mean difference -0.21% , $p = 0.04$) in patients, while reactivity to hypercapnia was preserved in the cortex, subcortical gray matter, and normal appearing white matter. Among patients, reactivity to hypercapnia was decreased in white matter hyperintensities compared to normal appearing white matter (BOLD mean difference -0.29% , $p = 0.02$).

Interpretation: Multiple aspects of cerebral small vessel function on 7T-MRI were abnormal in CADASIL patients, indicative of increased arteriolar stiffness and regional abnormalities in reactivity, locally also in relation to white matter injury. These observations provide novel markers of cSVD for mechanistic and intervention studies.

ANN NEUROL 2022;00:1–11

View this article online at [wileyonlinelibrary.com](https://onlinelibrary.wiley.com/doi/10.1002/ana.26527). DOI: 10.1002/ana.26527

Received May 12, 2022, and in revised form Oct 5, 2022. Accepted for publication Oct 7, 2022.

Address correspondence to Dr. Biessels, Department of Neurology and Neurosurgery, University Medical Center Utrecht, Heidelberglaan 100, Utrecht, 3508, GA, The Netherlands. E-mail: g.j.biessels@umcutrecht.nl

[†]These authors contributed equally to this work

From the ¹Department of Neurology and Neurosurgery, University Medical Center Utrecht Brain Center, University Medical Center Utrecht, Utrecht, The Netherlands; ²Institute for Stroke and Dementia Research, University Hospital, Ludwig-Maximilians-University Munich, Munich, Germany; ³Department of Radiology, Center for Image Sciences, University Medical Center Utrecht, Utrecht, The Netherlands; ⁴Spinoza Centre for Neuroimaging Amsterdam, Amsterdam, The Netherlands; ⁵Medical Image Analysis Center (MIAC AG) and qbig, Department of Biomedical Engineering, University of Basel, Basel, Switzerland; ⁶Brain Research Imaging Centre, Centre for Clinical Brain Sciences, UK Dementia Research Institute Centre at the University of Edinburgh, Edinburgh, UK; ⁷Institute of Psychiatry and Neurosciences of Paris, Université de Paris, Inserm U1266, Paris, France; ⁸Munich Cluster for Systems Neurology (SyNergy), Munich, Germany; and ⁹German Center for Neurodegenerative Disease (DZNE), Munich, Germany

Additional supporting information can be found in the online version of this article.

© 2022 The Authors. *Annals of Neurology* published by Wiley Periodicals LLC on behalf of American Neurological Association. 1
This is an open access article under the terms of the [Creative Commons Attribution-NonCommercial-NoDerivs](https://creativecommons.org/licenses/by-nc-nd/4.0/) License, which permits use and distribution in any medium, provided the original work is properly cited, the use is non-commercial and no modifications or adaptations are made.

Introduction

Cerebral small vessel diseases (cSVDs) are a major cause of stroke and dementia.¹ cSVD related lesions on brain MRI can be found in roughly 70% of 65-year-old individuals and in almost all 90-year-olds.² Despite the profound health impact of cSVDs, there is no specific treatment, likely due to our limited understanding of underlying disease mechanisms. Because of the small diameter of affected blood vessels in cSVDs and the limited resolution of conventional techniques for *in vivo* imaging in humans, cSVDs have been mostly studied through markers of parenchymal injury (e.g., lacunes, white matter hyperintensities [WMH], microbleeds, enlarged perivascular spaces,³ microstructural white matter changes,^{4–6} blood based markers of neuro-axonal damage⁷). While these markers are important because of their association with major clinical outcomes including stroke, cognitive decline, and dementia, they represent downstream consequences of cSVDs. To understand underlying mechanisms of cSVDs, it is essential to study the disease at its core, the vessels themselves.

Cerebral Autosomal Dominant Arteriopathy with Subcortical Infarcts and Leukoencephalopathy (CADASIL) is a monogenic form of cSVD caused by mutations in the *NOTCH3* gene. Previous studies on the brain vasculature in CADASIL have been mostly restricted to the examination of autopsy material.^{8, 9} Pathology in pial and small perforating cerebral arteries is an important feature, including degeneration of vascular smooth muscle cells and thickening of the arteriolar wall.^{8–10} This likely has an impact on small vessel function, which has indeed been observed in pial and perforating arteries in experimental animal models^{11, 12} and also in small vessels outside of the brain in humans, for example in the heart.¹³ Ultra-high field imaging with 7T-MRI now provides *in vivo* measures that inform on several aspects of cerebral small vessel function in humans, including perforating artery flow velocity and stiffness, and endothelium dependent and independent vascular reactivity in different brain regions.^{14, 15} These measures may provide leads on disease mechanisms in CADASIL and other forms of cSVDs.

We set out to evaluate cerebral small vessel function in CADASIL patients using 7T-MRI. Specifically, we assessed which measures of small vessel function on 7T-MRI are affected in CADASIL patients compared with controls and if small vessel dysfunction on 7T-MRI is associated with WMH in CADASIL.

Methods

Study Design and Participants

Participants in this study were recruited through the ZOOM@SVDs study, a prospective observational cohort

study.¹⁵ At University Hospital Ludwig-Maximilians-University (LMU) Munich, 23 CADASIL patients and 13 individually age- and sex-matched controls were recruited between October 2017 and July 2019. CADASIL was either confirmed by mutation in the *NOTCH3* gene ($n = 20$) or by skin biopsy ($n = 3$). Controls were recruited among partners or relatives of the patients and through flyer advertisement. Participants underwent clinical assessment and 3T brain MRI at the LMU and travelled to the University Medical Center (UMC) Utrecht in the Netherlands to undergo 7T brain MRI. Participants travelled to Utrecht through their preferred means and were offered a 1 night stay in a hotel. All travel expenses were covered. Participants received no further financial compensation. Detailed inclusion and exclusion criteria and study procedures are published elsewhere.¹⁵

The Medical Ethics Review Committees of the LMU (Project Number 17-088) and UMC Utrecht (Project number NL62090.041.17) approved the study. Written informed consent was obtained from all participants. The study was registered in the Netherlands Trial Register; NTR6265.

Clinical Assessment

Demographics and vascular risk profiles were recorded for all participants. Stroke, hypertension, and diabetes mellitus were recorded based on presence in medical history. Current systolic and diastolic blood pressure were based on 7-day blood pressure measurements done three times a day at home with a telemetric blood pressure device (Tel-O-Graph[®] GSM Plus, graded A/A by the British Hypertension Society). Smoking was based on self-report.

3T Brain MRI

Participants underwent 3T brain MRI at the LMU on a Siemens Magnetom Skyra 3T scanner with a 64-channel head coil. The scan protocol included 3D T1-weighted gradient echo, 3D T2*-weighted multi-echo gradient echo, and 3D fluid-attenuated inversion recovery (FLAIR) scan (sequence details Table 1). Lacunes (on T1-weighted and FLAIR scan) and microbleeds (on longest echo time of T2*-weighted scan) were manually counted according to the STRIVE-criteria.¹⁶ Segmentations of WMH, lacunes, intracranial volume, and total brain volume, were assessed as previously published.¹⁷

7T Brain MRI

All participants underwent 7T-MRI at the UMC Utrecht (Philips Healthcare, Best, The Netherlands) using a 32-channel receive head coil with a quadrature transmit coil (Nova Medical, MA, USA) (sequence details

TABLE 1. Brain MRI Scan Parameters

MR Sequence	Acquired Resolution mm ³	Time min:s	Parameters
3T-MRI			
T1-weighted GE	1.0 × 1.0 × 1.0	05:08	FOV 256 × 256 × 192 mm ³ ; TR 2500 ms; TE 4.37 ms; TI 1100 ms; flip angle 7°
T2*-weighted GE	0.9 × 0.9 × 2.0	05:56	FOV 230 × 160 × 187 mm ³ ; TR 35 ms; TE 4.9–29.5 ms, deltaTE 4.9 ms; flip angle 15°
FLAIR	1.0 × 1.0 × 1.0	06:27	FOV 250 × 250 × 176 mm ³ ; TR 5000 ms; TE 398 ms; TI 1800 ms
7T-MRI			
T1-weighted	1.0 × 1.0 × 1.0	01:59	FOV 250 × 250 × 190 mm ³ ; TR 4.2 ms; TI 1297 ms; shot interval 3,000 ms; flip angle 5°
2D-Qflow CSO	0.3 × 0.3 × 2.0	03:24 ^c	FOV 230 × 230 mm ² ; reconstructed resolution 0.18 × 0.18mm ² ; TR 29 ms; TE 16 ms; Venc 4 cm/s; temporal resolution 116 ms; flip angle 50°
2D-Qflow BG	0.3 × 0.3 × 2.0	03:47 ^c	FOV 170 × 170 mm ² ; reconstructed resolution 0.18 × 0.18mm ² ; TR 28 ms; TE 15 ms; Venc 20 cm/s; temporal resolution 112 ms; flip angle 50°
BOLD visual cortex ^a	1.3 × 1.3 × 1.3	10:05	FOV 140 × 140 × 11 mm ³ ; TR 880 ms; TE 25 ms
BOLD whole-brain ^b	2.0 × 2.0 × 2.0	10:00	FOV 224 × 256 × 101 mm ³ ; TR 3000 ms; TE 25 ms

BG = basal ganglia; BOLD = blood-oxygen-level dependent; CSO = centrum semiovale; FOV = field of view; GE = gradient echo; TE = echo time; TI = inversion time; TR = repetition time.

^aThe participant is presented with a *short visual stimulus*.

^bThe participant undergoes a *hypercapnic challenge*. Between the two BOLD sequences the participant is taken out of the scanner for a short break and to put on the mask for the hypercapnic challenge.

^cTotal scan time for a heart rate of 80 bpm.

Table 1). Three complementary aspects of small vessel function were investigated.

1. 7T-MRI allows to assess blood flow velocity and pulsatility within perforating arteries at the level of the basal ganglia (known diameter 200–800 μm) and centrum semiovale (100–300 μm), indicative of perforating artery stiffness.^{18–20} Flow velocity data were acquired with two, single-slice 2D-Qflow velocity mapping acquisitions, and a peripheral pulse unit was used for retrospective cardiac gating. Mean blood flow velocity and pulsatility index in perforating arteries in the basal ganglia and centrum semiovale were calculated (see supplementary table for exact processing pipeline).
2. Reactivity in response to a short visual stimulus was assessed in the visual cortex with the blood-oxygen-level dependent (BOLD) response. Participants were

presented with a 8 Hz blue-yellow reversing checkerboard using very short (0.5 s) and long blocks (16.7 s) of visual stimulation, during a 10-min experiment (for detailed parameters see design paper¹⁵). Neuronal activation to these stimuli induces vasodilation via neurovascular coupling and signalling from capillaries to pre-capillary arterioles to increase blood flow to the activated cortex.²¹ The activation pattern in response to the long blocks of visual stimulation for each subject served as region of interest. The BOLD signal on 7T-MRI is weighted more towards signals from the microvasculature (e.g., capillaries, small venules) than on lower field strength,²² which allows us to measure BOLD reactivity in small vessels as long as the large pial veins are removed from the region of interest.¹⁵ In addition, the high temporal resolution on 7T-MRI provides a precise estimate of the hemodynamic

response function (HRF) within the region of interest in response to very short visual stimulation (see supplementary table for exact processing pipeline). The BOLD% signal change and full width at half maximum of the HRF estimate are the main outcome variables.

- Whole-brain reactivity to a hypercapnic stimulus was measured with the BOLD response. The participants wore a face mask to breathe medical air and premixed 6% CO₂ in air in alternating blocks: 3 x 2-min blocks of medical air with 2 x 2-min blocks of 6% CO₂ in air in between (for detailed parameters see design paper¹⁵). The hypercapnic stimulus causes relaxation of the vascular smooth muscle cells, primarily at the level of the arterioles, thereby causing endothelium independent small vessel vasodilation.^{23, 24} Monitoring equipment recorded pulse rate and end-tidal CO₂ (40 Hz, CD3-A AEI Technologies, Pittsburgh, PA, USA) (based on Thrippleton et al,²⁵ as specified in van den Brink et al¹⁵). Signal from large pial veins was again excluded so the remaining BOLD signal primarily represents small vessel reactivity (see supplementary table for exact processing pipeline). The high spatial resolution of BOLD on 7T-MRI permits regional analyses. The BOLD% signal change in the cortical gray matter, sub-cortical gray matter, and white matter are the main outcome measures.

The order of MRI scans was strictly adhered to. After the first BOLD scan with visual stimulation, every participant was taken out of the scanner. After a short break of at least 5 minutes, the participant put on the breathing mask and the protocol was continued with the hypercapnic challenge.

Statistical Analysis

Differences in characteristics between CADASIL patients and controls were tested with an independent samples *t*-test for continuous normally distributed data, Mann–Whitney *U* test for non-parametric continuous data and chi-square for categorical data. Differences between patients and controls in small vessel function measures were tested with analysis of covariance (ANCOVA). Age and sex were included as a covariate to accommodate small differences in age and sex between groups. Pulsatility index was additionally corrected for mean blood flow velocity, and BOLD hypercapnia comparisons were additionally corrected for change in end-tidal CO₂ in response to hypercapnia.

Within the patient group, mean blood flow velocity and pulsatility index in the perforating arteries in the centrum semiovale and BOLD% signal change to

hypercapnia were compared in normal appearing white matter (NAWM) and WMH with a paired *t*-test. This comparison could not be made for perforating arteries in the basal ganglia because of limited WMH volume in that region of interest. For the same reason NAWM versus WMH comparisons for BOLD% signal change to hypercapnia could not be performed in control participants.

For measures of small vessel function that differed between patients and controls we performed explorative analyses in the patient group, where we related these measures to age and WMH volume. WMH volume was normalized to the intracranial volume and because data were skewed, we used the cube-root of the WMH volume. Given the collinearity of possible confounders (e.g., age relates to disease stage) with small vessel function measures, we did not correct for possible confounding variables in these explorative analyses.

All statistical analyses were performed in SPSS version 25 and *p* < 0.05 was considered significant.

Results

The characteristics of the 23 CADASIL patients and 13 controls are shown in Table 2. Groups were reasonably well matched with respect to age and sex (patients: mean age 51.1 ± 10.1 years, 52% female; controls: 46.1 ± 12.6 years, 46% female). As expected, patients more often had a history of stroke, more often used anti-platelet drugs, and showed high burden of imaging markers of cSVD on 3T-MRI. None of the controls was excluded because of covert cSVD on MRI (i.e., presence of lacunes or Fazekas ≥ 2 as defined in the protocol¹⁵), as expected given their age. Figure 1 lists the number of 7T measures included in the final analysis. Participants with missing or failed 7T measurements were no different regarding demographics or disease severity than participants with complete 7T datasets.

Small Vessel Function in CADASIL Patients and Controls

Perforating Artery Flow Velocity and Pulsatility. Perforating artery density (i.e., number of perforating arteries per cm² of the subject specific region of interest) was similar in patients and controls both in the centrum semiovale (2.2 ± 0.8/cm² and 2.2 ± 1.0/cm² respectively, *p* = 0.86) and the basal ganglia (0.9 ± 0.3/cm² and 1.0 ± 0.3/cm², *p* = 0.33). Figure 2A,C display the mean blood flow velocity in perforating arteries in the centrum semiovale and basal ganglia respectively for CADASIL patients and controls (see Figure 2B and 2D for individual traces). Mean perforating artery blood flow velocity was lower, and pulsatility index higher in CADASIL patients than in controls, both in the centrum semiovale and basal

TABLE 2. Characteristics of CADASIL Patients and Controls

	CADASIL n = 23	Control n = 13	p-Value
Demographics			
Age, M ± SD	51.1 ± 10.1	46.1 ± 12.6	0.20
Female sex, n (%)	12 (52)	6 (46)	1.00
Vascular risk profile			
Stroke, n (%)	7 (30)	0 (0)	0.03
Hypertension, n (%)	4 (17)	1 (8)	0.63
Current 7-day systolic BP, M ± SD [mmHg]	118.4 ± 10.1	120.9 ± 10.2	0.48
Current 7-day diastolic BP, M ± SD [mmHg]	76.0 ± 8.9	79.0 ± 10.6	0.37
Diabetes Mellitus, n (%)	0 (0)	1 (8)	0.36
Current/ever smoker, n (%)	15 (65)	6 (46)	0.31
Medication use			
Antihypertensives, n (%)	6 (26)	1 (7)	0.23
Statins, n (%)	9 (39)	1 (7)	0.06
Antiplatelet drugs, n (%)	14 (61)	1 (7)	0.004
3T-MRI SVD markers			
WMH volume, median [min-Q1-Q3-max] [% of ICV]	3.87 [0.88–2.06–5.56–7.89]	0.01 [0.00–0.00–0.03–0.12]	<0.001
Lacune presence, n (%)	13 (57)	0 (0)	0.001
Lacune count ^a , median [Q1-Q3]	4 [3–8]	0 [0–0]	
Microbleed presence, n (%)	13 (57)	0 (0)	0.001
Microbleed count ^b , median [Q1-Q3]	3 [2–8]	0 [0–0]	
Brain volume, M ± SD [% of ICV]	78.3 ± 5.2	77.6 ± 3.2	0.76

BP = blood pressure; M = mean; ICV = intracranial volume; SD = standard deviation; WMH = white matter hyperintensities; Q1-Q3 = quartile 1 and quartile 3.

^aCount for participants with ≥1 lacune(s).

^bCount for participants with ≥1 microbleed(s).

ganglia (Table 3). When only perforating arteries in the NAWM were considered, differences between patients (blood flow velocity 0.55 ± 0.07 cm/s and pulsatility index 0.62 ± 0.24) and controls (blood flow velocity 0.63 ± 0.13 cm/s and pulsatility index 0.37 ± 0.11) were similar ($p = 0.05$ and $p = 0.01$, respectively). Among CADASIL patients perforating artery flow velocity and pulsatility were similarly affected in WMH (blood flow velocity 0.48 ± 0.14 cm/s and pulsatility index 0.85 ± 0.45) and NAWM (blood flow velocity 0.53 ± 0.06 cm/s and 0.60 ± 0.28 , $p = 0.14$ and $p = 0.07$, respectively).

Small Vessel Reactivity in Response to a Visual Stimulus

Figure 2E displays the mean estimate of the HRF to a visual stimulus in the visual cortex in CADASIL patients and controls respectively (see Figure 2F for individual traces). Of note, the size (i.e., number of activated voxels) of the participant-specific regions of interest in which the HRFs were estimated was similar between patients (percentage activated voxels in scanning plane: 32.7 ± 13.3) and controls (30.4 ± 12.7 , $p = 0.54$). The peak BOLD% signal change was lower in patients compared with controls (Table 3). There was no significant group difference

	2D-Qflow centrum semiovale		2D-Qflow basal ganglia		BOLD short visual stimulus		BOLD hypercapnia	
	CADASIL	Control	CADASIL	Control	CADASIL	Control	CADASIL	Control
	23	13	23	13	23	13	23	13
Measurement not acquired	↓ ₀	↓ ₁	↓ ₀	↓ ₁	↓ ₁	↓ ₀	↓ ₄	↓ ₁
	23	12	23	12	22	13	19	12
Technically failed measurement	↓ ₀	↓ ₁	↓ ₂	↓ ₁	↓ ₁	↓ ₁	↓ ₂	↓ ₁
	23	11	21	11	21	12	17	11
Movement	↓ ₁	↓ ₁	↓ ₀	↓ ₂	↓ ₂	↓ ₂	↓ ₀	↓ ₀
	22	10	21	9	19	10	17	11

Figure 1: Flowchart showing reasons for excluded scans per small vessel function measure. Reasons for not acquired measurements are: technical failure on the scanner for the 2D-Qflow scans, glasses that would not fit in the head coil for the blood-oxygen-level dependent (BOLD) short visual stimulus scan, and participants unwilling or unable to do the hypercapnia challenge after first trying it outside the scanner for the BOLD hypercapnia scan.

in response timing parameters; full width at half maximum (Table 3), onset time (patients 2.10 ± 0.54 s; controls 1.72 ± 0.46 s, $p = 0.09$), and time-to-peak (4.62 ± 1.04 s; 4.39 ± 0.38 s, $p = 0.46$).

Whole-Brain Small Vessel Reactivity to a Hypercapnic Stimulus

There were no significant group differences in BOLD% signal change to hypercapnia in any of the regions of interest (Table 3). When looking in more detail, BOLD% signal change was non-significantly higher in the cortical gray matter, total white matter, and NAWM in patients versus controls (Table 3). In patients, BOLD% signal change was lower in WMH (0.24 ± 0.40) than NAWM (0.53 ± 0.54 , $p = 0.02$).

Small Vessel Function and Age and WMH Volume in CADASIL Patients

Relations with age and WMH volume were explored for 7T measures that were affected in patients. There was a trend for a negative association between blood flow velocity within perforating arteries of the centrum semiovale and WMH volume but not age (Table 4). There was no relation between small vessel function measures and antiplatelet or antihypertensive drug use (all $p > 0.05$).

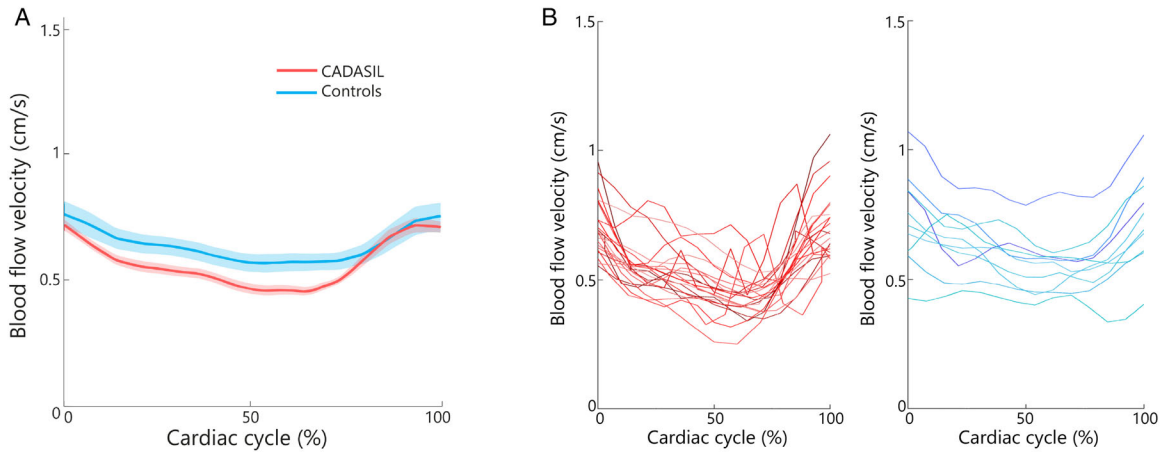
Discussion

This study found multiple abnormalities of cerebral small vessel function in CADASIL, in a well-defined sample of prospectively recruited patients and controls, applying cutting-edge 7T-MRI technology. These abnormalities involved between group differences in blood flow velocity and pulsatility in perforating arteries, as well as in reactivity to a visual or hypercapnic stimulus, likely reflecting changes in vascular physiology in multiple small vessel

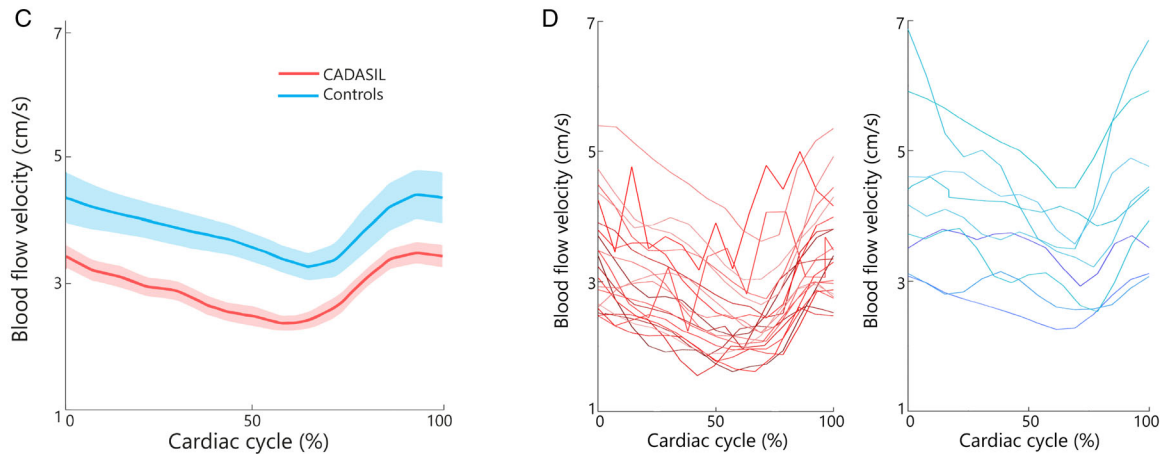
populations. Moreover, among patients, cortical reactivity to a hypercapnic stimulus locally associated to white matter injury.

Reduced mean flow velocity and increased pulsatility in CADASIL patients were observed in perforating arteries both in the basal ganglia, fed by proximal intracranial arteries, and the centrum semiovale, fed by distal arterial branches. Only one previous study also reported decreased blood flow velocity in perforating arteries in CADASIL,²⁶ albeit in the most proximal section of the lenticulostriate arteries, that have a larger diameter than the perforating arteries in our current work. We previously assessed our 7T-MRI measures of perforating artery flow velocity in a small explorative study in patients with sporadic cSVDs (i.e., with lacunar infarction or deep intracerebral haemorrhage) and observed increased pulsatility in patients compared to controls but no reduction in flow velocity.¹⁹ Decreased blood flow velocity on 2D-Qflow velocity measures can be explained by decreased total blood flow or increase in arteriolar lumen area. The perforating arteries that we assess have a sub-voxel size diameter. Therefore, we cannot actually measure lumen area or total blood flow. Of note, a previous autopsy study in CADASIL showed that lumen diameter is unchanged in the basal ganglia, but is decreased due to intimal thickening and fibrosis in perforating arteries in the white matter.²⁷ Therefore, given the current understanding of the disease,²⁸ decreased blood flow velocity in CADASIL is likely attributable to decreased total blood flow in the perforating arteries. Of note, flow velocity and pulsatility index in the perforating arteries are not independent of effects up- and downstream in the vascular tree.²⁹ Increased pulsatility index of perforating artery flow velocity may therefore reflect changes in upstream vessels (generating a more pulsatile perfusion pressure), enhanced

Blood flow velocity in centrum semiovale perforating arteries



Blood flow velocity in basal ganglia perforating arteries



Hemodynamic response function

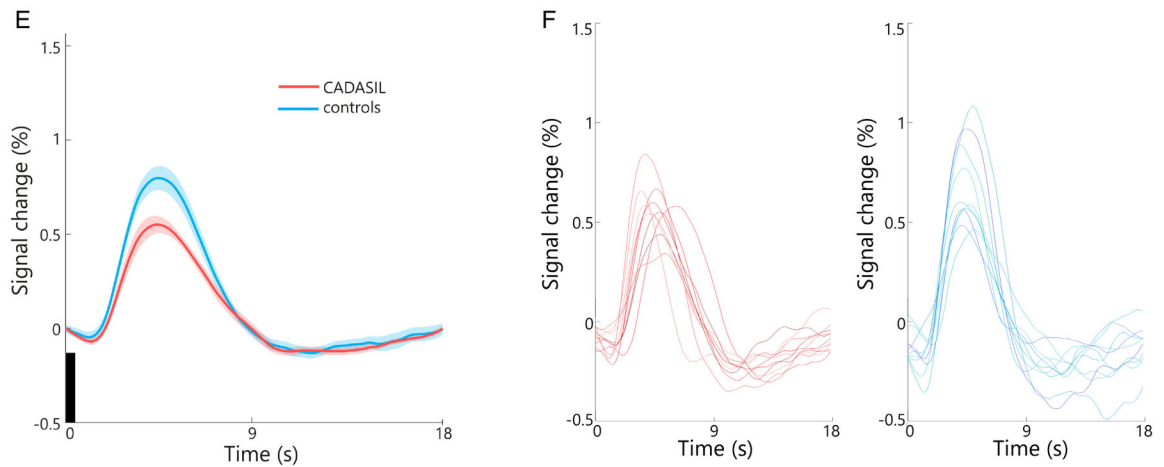


Figure 2: Mean and individual participant traces. The mean blood flow velocity (solid lines) and standard errors of the mean (shaded lines) in perforating arteries in the centrum semiovale (A) and basal ganglia (C) for Cerebral Autosomal Dominant Arteriopathy with Subcortical Infarcts and Leukoencephalopathy (CADASIL) patients and controls. Individual blood flow velocity traces in perforating arteries in the centrum semiovale (B) and basal ganglia (D) for CADASIL patients in red and controls in blue. (E) The mean hemodynamic response function estimates (solid lines) and standard errors of the mean (shaded areas) after 500 ms visual stimulation (black bar) for CADASIL patients and controls. (F) Individual BOLD hemodynamic response function estimates after 500 ms visual stimulation for all CADASIL patients in red and controls in blue.

stiffness of the pial or perforating arteries themselves, or changes in the downstream vascular bed including abnormal microvascular compliance. Autopsy studies in CADASIL have reported vessel changes primarily in arterioles, but also in capillaries and venules.^{28, 30, 31} In addition to luminal narrowing in white matter arterioles, these changes include degeneration of smooth muscle cells and reduced capillary length. Moreover, although changes in small vessel function have been noted outside of the brain in CADASIL (for example in the heart¹³), indicating systemic effects of the disease, systemic perfusion pressure as reflected in blood pressure and pulse pressure, was not affected in our patients. Hence, upstream changes in larger vessels are unlikely to explain increased pulsatility in CADASIL. It seems more likely that increased pulsatility reflects vascular stiffness of the perforating arteries at the point that they are probed with the 7T measurements or downstream small arterioles. Of note, blood flow velocity and pulsatility index changes in perforating arteries in NAWM and WMH were similar. Hence, the observed changes likely reflect generalized disease effects on these

perforating arteries, although it should be considered that 2D slices predominantly capture perforating arteries that are passing through the white matter at the site of measurement rather than arteries that specifically supply the white matter contained in the slice. Finally, we found indications that blood flow velocity in perforating arteries of the centrum semiovale associates negatively with WMH volume, suggesting that these measures may become progressively abnormal in patients as the disease evolves.

Both measures of small vessel reactivity were affected in CADASIL patients. The neurovascular coupling dependent response to a short visual stimulus elicited lower reactivity in the visual cortex in patients compared with controls. Additionally, reactivity to hypercapnia, which acts directly on vascular smooth muscle cells in arterioles, was decreased in WMH compared to NAWM in patients. Similar to our result, decreased reactivity within WMH to hypercapnia and acetazolamide was a consistent finding in earlier studies in CADASIL that were conducted at lower field strength.^{32, 33} We did observe non-significant higher

TABLE 3. Small Vessel Function on 7T-MRI in CADASIL Patients and Controls

	CADASIL	Control	<i>p</i> -Value
2D-Qflow centrum semiovale^a	n = 22	n = 10	
Blood flow velocity [cm/s]	0.54 ± 0.06	0.63 ± 0.13	0.03
Pulsatility index ^b	0.57 ± 0.19	0.37 ± 0.11	0.009
2D-Qflow basal ganglia^a	n = 21	n = 9	
Blood flow velocity [cm/s]	3.07 ± 0.67	4.05 ± 0.83	0.003
Pulsatility index ^b	0.46 ± 0.12	0.29 ± 0.15	0.06
BOLD short visual stimulus^c	n = 19	n = 10	
BOLD % signal change	0.61 ± 0.20	0.82 ± 0.25	0.04
Full width at half max [s]	3.82 ± 0.65	3.94 ± 0.36	0.59
BOLD hypercapnic stimulus^d	n = 17	n = 11	
CGM BOLD % signal change	3.66 ± 1.24	3.07 ± 1.20	0.26
SGM BOLD % signal change	3.37 ± 0.98	3.45 ± 1.43	0.77
WM BOLD % signal change	0.35 ± 0.33	0.17 ± 0.31	0.31
NAWM BOLD % signal change	0.53 ± 0.54	0.17 ± 0.31	0.18

BOLD = blood-oxygen-level dependent; CGM = cortical gray matter; NAWM = normal appearing white matter; SGM = subcortical gray matter; WM = white matter.

Data are shown as mean ± standard deviation.

^aThe region of interest is the entire centrum semiovale and basal ganglia excluding lacunes. Analyses are corrected for age and sex.

^bAdditional correction for blood flow velocity.

^cAnalyses corrected for age and sex.

^dAnalyses corrected for age, sex and change in end-tidal CO₂ to hypercapnia.

TABLE 4. Associations of Small Vessel Dysfunction with Age and WMH Volume in CADASIL Patients

	Age	WMH Volume
2D-Qflow centrum semiovale^a		
Blood flow velocity (cm/s)	B = -51.25 <i>p</i> = 0.15	B = -0.57 <i>p</i> = 0.05
Pulsatility index	B = -9.62 <i>p</i> = 0.42	B = -0.10 <i>p</i> = 0.35
2D-Qflow basal ganglia^a		
Blood flow velocity (cm/s)	B = -1.44 <i>p</i> = 0.69	B = -0.04 <i>p</i> = 0.18
Pulsatility index	B = 26.23 <i>p</i> = 0.20	B = 0.13 <i>p</i> = 0.48
BOLD short visual stimulus		
BOLD % signal change	B = -2.17 <i>p</i> = 0.87	B = -0.04 <i>p</i> = 0.70
BOLD hypercapnic stimulus		
WMH BOLD % signal change	B = -2.46 <i>p</i> = 0.74	B = 0.01 <i>p</i> = 0.87

BOLD = blood-oxygen-level dependent; CGM = cortical gray matter; WMH = white matter hyperintensities.

Note: Tested with linear regression without corrections. WMH volume was normalized for intracranial volume and cube-root transformed. Sensitivity analyses on non-transformed data, with Spearman correlations, produced similar results (data not shown).

^aThe region of interest is the entire centrum semiovale and basal ganglia minus lacunes.

reactivity to hypercapnia in the cortical gray matter, total white matter, and NAWM in patients compared with controls. Whether this finding across these three different regions represents a true phenomenon or is due to chance remains to be determined, as earlier studies have not reported such results.^{32, 33} On the other hand, *increased* cortical reactivity in the visual cortex was reported in CADASIL patients versus controls in a study that used visual stimulation, with a much longer stimulus (40 s),³⁴ compared to our study (0.5 s). These differential findings

are likely the result of fundamental differences in the nature and duration of the stimuli. Clearly, responses to different types of stimuli involve different physiological pathways in different vessel populations. The BOLD signal to a visual stimulus depends on neurovascular coupling, entailing activation of cortical neurons, which directly initiates an endothelium dependent response of local capillaries and upstream feeding arterioles. Hypercapnia, on the other hand, is a stimulus that according to current insight directly affects smooth muscle cells in the arterioles throughout the brain, in an endothelial independent manner.²³ In addition, the differences in stimulus duration between different paradigms will have an effect on the BOLD signal as well. Short stimuli (<1 second, e.g., short visual stimulation) only engage blood flow changes via arteriole dilation. In contrast, prolonged stimuli (e.g., 2 minute hypercapnia) also induce notable blood volume changes on the venous side that will affect the BOLD signal as well.³⁵ Therefore, different stimulus durations will also probe different vascular pools and thus assess vascular reactivity and signals of different vessel populations. Our findings thus suggest that in CADASIL patients the vascular system is unable to sufficiently respond to quick, subtle and local demands in the cortex. In contrast, prolonged and global stimulation by hypercapnia can still generate vascular responses, resulting in a preserved response in the cortex, although not in WMH.

Taken together, these findings suggest that changes in small vessel blood flow velocity, pulsatility and reactivity in CADASIL patients depend on the tissue type that is assessed and the type and extent of stimulation. This likely reflects the dynamic nature of small vessel function. These findings warrant further studies, also with longitudinal design and also involving patients with sporadic cSVDs. It would be of particular interest to explore if these measures of small vessel function respond to drug therapy and as such could serve as an intermediate outcome measure in future cSVD drug trials. Reactivity to hypercapnia at 3T-MRI is already evaluated in that context.³⁶ Yet, for the novel more detailed 7T-MRI measures presented here this will first require further characterisation.

A strength of our study is that we used three measures that probe complementary aspects of small vessel function in one patient population. The advantage of 7T-MRI is that it provides high spatial and temporal resolution, but also enhances BOLD signal properties improving signal to noise and permitting separation of the signal in small vessels from that in larger draining veins.³⁷ Additionally, investigating a pure, genetically-defined disease like CADASIL enables to study cSVD without confounding factors associated with aging. A limitation of our study is potential selection bias inherent to the relatively

demanding study protocol, which required participants to travel from Germany to the Netherlands for 7T brain MRI. As a consequence, patients in this study were mostly in earlier disease stages with relatively limited lesion load and cognitive problems. This limited the possibilities to study the relation of small vessel function with markers of disease severity. On the other hand, the study shows that even in early stages, small vessel function changes are already apparent. In addition, the control group was age-matched and thus relatively young as well, with low burden of cSVD, which may have increased the contrasts between groups. Another limitation of the visual stimulus method is its dependence on an intact cortical neuronal response to the visual stimulus. Although we did not test this neuronal response in our study, it was previously shown to be unaffected in CADASIL patients.³⁴ Last, the temporal resolution of the Qflow sequences was relatively low, which could cause for an underestimation of the pulsatility index. The temporal resolution however needs to be balanced with a tolerable scan time³⁸ and we can still reliably study relative differences between patients and controls.

In conclusion, multiple aspects of cerebral small vessel function on 7T-MRI were abnormal in CADASIL patients, indicative of increased arteriolar stiffness and regional abnormalities in reactivity, locally also in relation to white matter injury. These abnormalities likely reflect dynamic changes in vascular physiology in multiple small vessel populations. These novel functional markers help to better understand disease mechanisms in CADASIL, but are likely also important for sporadic cSVDs.

Acknowledgments

ZOOM@SVDs is part of SVDs@target that has received funding from the European Union's Horizon 2020 research and innovative program under grant agreement No. 666,881. This work is also supported by Vici Grant 918.16.616 from the Netherlands Organisation for Scientific Research (NWO) to GJB. MDi has received funding from the Vascular Dementia Research Foundation, the LMUExcellent Investitionsfond, and the DFG as part of the Munich Cluster for Systems Neurology (EXC 2145 SyNergy –ID 390,857,198). JJMZ has received funding from the European Research Council under the European Union's Seventh Framework Program (FP/2007–2013) / ERC Grant Agreement n. 337333 and n. 841865. JMW is supported by the UK Dementia Research Institute which receives its funding from DRI Ltd, funded by the UK Medical Research Council, Alzheimer's Society and Alzheimer's Research UK, and the British Heart Foundation Centre for Research Excellence Award III (RE/18/5/34216).

Author Contributions

J.H., J.M.W., A.J., M.Di., and G.J.B. contributed to the conception and design of the study; Hvd.B., A.K., T.A., L.O., J.C.W.S., J.J.M.Z., S.H., M.H., B.G., M.Due., and M.S.S. contributed to the acquisition and analysis of data; Hvd.B., A.K., M.Di., and G.J.B. contributed to drafting the text or preparing the figures.

Potential Conflicts of Interest

The authors declare no conflicts of interest.

References

1. Wardlaw JM, Smith C, Dichgans M. Small vessel disease: mechanisms and clinical implications. *Lancet Neurol* 2019;18:684–696.
2. Dabette S, Schilling S, Duperron MG, et al. Clinical significance of magnetic resonance imaging markers of vascular brain injury: a systematic review and meta-analysis. *JAMA Neurol* 2019;76:81–94.
3. Wardlaw JM, Smith EE, Biessels GJ, et al. Neuroimaging standards for research into small vessel disease and its contribution to ageing and neurodegeneration. *Lancet Neurol* 2013;12:822–838.
4. van Norden AG, de Laat KF, van Dijk EJ, et al. Diffusion tensor imaging and cognition in cerebral small vessel disease: the RUN DMC study. *Biochim Biophys Acta* 2012;1822:401–407.
5. Tuladhar AM, van Norden AG, de Laat KF, et al. White matter integrity in small vessel disease is related to cognition. *NeuroImage Clin* 2015;7:518–524.
6. Baykara E, Gesierich B, Adam R, et al. A novel imaging marker for small vessel disease based on Skeletonization of white matter tracts and diffusion histograms. *Ann Neurol* 2016;80:581–592.
7. Duering M, Konieczny MJ, Tiedt S, et al. Serum neurofilament light chain levels are related to small vessel disease burden. *J Stroke* 2018;20:228–238.
8. Chabriat H, Joutel A, Dichgans M, et al. Cadasil. *Lancet Neurol* 2009;8:643–653.
9. di Donato I, Bianchi S, De Stefano N, et al. Cerebral autosomal dominant Arteriopathy with subcortical infarcts and leukoencephalopathy (CADASIL) as a model of small vessel disease: update on clinical, diagnostic, and management aspects. *BMC Med* 2017;15:1–12.
10. Hervé D, Chabriat H. CADASIL. *J Geriatr Psychiatry Neurol* 2010;23:269–276.
11. Joutel A, Monet-leprêtre M, Gosele C, et al. Cerebrovascular dysfunction and microcirculation rarefaction precede white matter lesions in a mouse genetic model of cerebral ischemic small vessel disease. *J Clin Invest* 2010;120:433–445.
12. Dabertrand F, Krøigaard C, Bonev AD, et al. Potassium channelopathy-like defect underlies early-stage cerebrovascular dysfunction in a genetic model of small vessel disease. *Proc Natl Acad Sci* 2015;112:E796–E805.
13. Argirò A, Sciarà R, Marchi A, et al. Coronary microvascular function is impaired in patients with cerebral autosomal dominant arteriopathy with subcortical infarcts and leukoencephalopathy. *Eur J Neurol* 2021;28:3809–3813.
14. Zwanenburg JJM, Van Osch MJP. Targeting cerebral small vessel disease with MRI. *Stroke* 2017;48:3175–3182.
15. van den Brink H, Kopczak A, Arts T, et al. Zooming in on cerebral small vessel function in small vessel diseases with 7T MRI: rationale and design of the “ZOOM@SVDs” study. *Cereb Circ—Cogn Behav* 2021;2:100013.

16. Wardlaw JM, Smith EE, Biessels GJ, et al. Neuroimaging standards for research into small vessel disease and its contribution to ageing and neurodegeneration. *Lancet Neurol* 2013;12:822–838.
17. Gesierich B, Tuladhar AM, ter Telgte A, et al. Alterations and test-retest reliability of functional connectivity network measures in cerebral small vessel disease. *Hum Brain Mapp* 2020;41:2629–2641.
18. Bouvy WH, Geurts LJ, Kuijff HJ, et al. Assessment of blood flow velocity and pulsatility in cerebral perforating arteries with 7-T quantitative flow MRI. *NMR Biomed* 2015;29:1295–1304.
19. Geurts L, Zwanenburg JJM, Klijn CJM, et al. Higher Pulsatility in cerebral perforating arteries in patients with small vessel disease related stroke, a 7T MRI study. *Stroke* 2019;50:62–68.
20. Arts T, Siero JCW, Biessels GJ, Zwanenburg JJM. Automated assessment of cerebral arterial perforator function on 7T MRI. *J Magn Reson Imaging* 2021;53:234–241.
21. Iadecola C. The neurovascular unit coming of age: a journey through neurovascular coupling in health and disease. *Neuron* 2017;96:17–42.
22. Uludağ K, Müller-Bierl B, Uğurbil K. An integrative model for neuronal activity-induced signal changes for gradient and spin echo functional imaging. *Neuroimage* 2009;48:150–165.
23. Ainslie PN, Duffin J. Integration of cerebrovascular CO₂ reactivity and chemoreflex control of breathing: mechanisms of regulation, measurement, and interpretation. *Am J Physiol - Regul Integr Comp Physiol* 2009;296:R1473–R1495.
24. Sleight E, Stringer MS, Marshall I, et al. Cerebrovascular reactivity measurement using magnetic resonance imaging: a systematic review. *Front Physiol* 2021;12:643468.
25. Thrippleton MJ, Shi Y, Blair G, et al. Cerebrovascular reactivity measurement in cerebral small vessel disease: rationale and reproducibility of a protocol for MRI acquisition and image processing. *Int J Stroke* 2018;13:195–206.
26. Sun C, Wu Y, Ling C, et al. Reduced blood flow velocity in lenticulostriate arteries of patients with CADASIL assessed by PC-MRA at 7T. *J Neurol Neurosurg Psychiatry* 2021;0:1–3.
27. Miao Q, Paloneva T, Tuisku S, et al. Arterioles of the lenticular nucleus in CADASIL. *Stroke* 2006;37:2242–2247.
28. Craggs LJJ, Yamamoto Y, Deramecourt V, Kalaria RN. Microvascular pathology and morphometrics of sporadic and hereditary small vessel diseases of the brain. *Brain Pathol* 2014;24:495–509.
29. Arts T, Onkenhout LP, Amier RP, et al. Non-invasive assessment of damping of blood flow velocity Pulsatility in cerebral arteries with MRI. *J Magn Reson Imaging* 2022;55:1785–1794.
30. Rajani RM, Ratelade J, Domenga-Denier V, et al. Blood brain barrier leakage is not a consistent feature of white matter lesions in CADASIL. *Acta Neuropathol Commun* 2019;7:1–14.
31. Pettersen JA, Keith J, Gao F, et al. CADASIL accelerated by acute hypotension: arterial and venous contribution to leukoariosis. *Neurology* 2017;88:1077–1080.
32. Chabriat H, Pappata S, Ostergaard L, et al. Cerebral hemodynamics in CADASIL before and after acetazolamide challenge assessed with MRI bolus tracking. *Stroke* 2000;31:1904–1912.
33. Atwi S, Shao H, Crane DE, et al. BOLD-based cerebrovascular reactivity vascular transfer function isolates amplitude and timing responses to better characterize cerebral small vessel disease. *NMR Biomed* 2019;32:1–12.
34. Cheema I, Switzer AR, McCreary CR, et al. Functional magnetic resonance imaging responses in CADASIL. *J Neurol Sci* 2017;375:248–254.
35. Uludağ K, Blinder P. Linking brain vascular physiology to hemodynamic response in ultra-high field MRI. *Neuroimage* 2018;168:279–295.
36. Blair GW, Janssen E, Stringer MS, et al. Effects of Cilostazol and Isosorbide Mononitrate on cerebral hemodynamics in the LACI-1 randomized controlled trial. *Stroke* 2022;53:29–33.
37. Siero JCW, Bhogal A, Jansma JM. Blood oxygenation level-dependent/functional magnetic resonance imaging: underpinnings, practice, and perspectives. *PET Clin* 2013;8:329–344.
38. Geurts L, Biessels GJ, Luijten P, Zwanenburg J. Better and faster velocity pulsatility assessment in cerebral white matter perforating arteries with 7T quantitative flow MRI through improved slice profile, acquisition scheme, and postprocessing. *Magn Reson Med* 2018;79:1473–1482.